Mechanism Behind Separation of Single-Walled Carbon Nanotubes *via* Density Gradient Ultracentrifugation Using Co-Surfactant Dispersions

Pei Zhao[†], *Erik Einarsson*[†‡], *Georgia Lagoudas*[§], *Junichiro Shiomi*[†], *Shohei Chiashi*[†], *Shigeo Maruyama*[*,†]

[†]Department of Mechanical Engineering, The University of Tokyo

7-3-1 Hongo, Bunkyo-ku, Tokyo 113-8656, Japan

[‡]Global Center of Excellence for Mechanical Systems Innovation, The University of Tokyo

7-3-1 Hongo, Bunkyo-ku, Tokyo 113-8656, Japan

[§]Department of Bioengineering, Rice University

6100 Main Street, Houston, Texas 77005, USA

*Author email: maruyama@photon.t.u-tokyo.ac.jp

ABSTRACT. As one of the most promising and effective techniques to separate single-walled carbon nanotubes (SWNTs), the density gradient ultracentrifugation (DGU) method is widely used to obtain SWNTs with desired chiralities, diameters, or electronic types. We report modifications to this surfactant-assisted technique that result in continuous tuning of diameter-dependent separation and/or electronic-type separation of SWNTs by adjusting the co-surfactant dispersion conditions. The resulting buoyant densities, layer positions, and optical absorbance information of successive separated layers were analyzed, and the results suggest that the surfactant hydration conditions, affinities to SWNTs, and surrounding environment determine the exchange process between different surfactants when using bile salts such as *sodium deoxycholate* (DOC) and anionic salts like *sodium dodecyl sulfate* (SDS). These properties also determine the adsorption morphologies and the buoyancies of resulting surfactant-SWNT micelles. The model described here explains these experimental results, and can help design new DGU experiments by predicting outcomes of different starting recipes.

KEYWORDS: Single-walled carbon nanotubes, Density gradient ultracentrifugation, Surfactant

The one-dimensional structure of single-walled carbon nanotubes (SWNTs) imparts on them a variety of remarkable physical, chemical and biological properties. Due to these numerous desirable characteristics, SWNTs have potential for use in a wide range of applications including electronics, optics, and biosensors.[1] However, since the electrical nature of an SWNT is structure-dependent, their widespread use in applications will remain limited until homogeneous SWNTs can be obtained in sufficient quantities. Direct synthesis of homogeneous SWNTs is of course the most desirable method to achieve this, but current methods of production cannot produce homogeneous SWNTs. Various separation methods have been developed over the last few years to obtain small amounts of SWNTs with a specific chirality or electronic type.[2-20] Of all these techniques, the density gradient ultracentrifugation (DGU) method, adapted to SWNTs by Arnold *et al*.,[6,7] is considered one of the most promising and effective for achieving good SWNT selectivity not only by electronic type[7,11-14] but also diameter[7,15-20] and even chirality.[7,18-20]

Generally speaking, in the DGU method SWNTs are suspended in water by dispersing with a surfactant, which forms a micelle around the SWNTs. Different wrapping morphologies form micelles of different sizes and densities, and DGU is used to separate the surfactant-wrapped SWNTs based on these small density differences. The choices of surfactants and density gradient profile turn out to be very important, with the former playing the most critical role. Additionally, dual-surfactant recipes have been the most effective in isolating SWNTs.[7,20]

The most commonly used surfactants in DGU are anionic salts such as *sodium dodecyl sulfate* (SDS) and bile salts such as *sodium deoxycholate* (DOC) or *sodium cholate* (SC). These surfactants have different affinities to different SWNTs because of their specific molecular structures.[21,22] This results in surfactant wrapping that is dependent on the SWNT structure or electronic type. Several explanations of this wrapping have been proposed, and various theoretical calculations,[23] numerical simulations,[15,24,25] neutron scattering measurements[26], and observations by transmission electron microscopy (TEM)[27] have been performed. The separation mechanism, however, has yet to be clarified.

In this work, we propose a model that describes the underlying mechanism resulting in various SWNT separations by different DGU processes including diameter-dependent separation, electronic type separation, and simultaneous separation of both types. This mechanism is an extension of our recent investigation of diameter-dependent separation by DGU,[19] and is supported by our new experimental results as well as those reported by others. The results were obtained using various processes involving aqueous SWNT solutions dispersed by co-surfactant agents DOC and SDS. By comparing the pre-DGU recipes and post-DGU information such as buoyant densities, layer positions and absorbance spectral shifts, we clarify the role of the different surfactants used to obtain separation of SWNTs by DGU.

Results and Discussion

In order to clarify the mechanism behind co-surfactant DGU separation of SWNTs we analyzed the outcomes of DGU separations resulting from various processes. We investigated the influence and role of co-surfactants DOC and SDS by dispersing SWNTs in either one or two stages prior to DGU. In the former case both surfactants were used simultaneously for the initial dispersion, while in the latter case DOC was used for the initial dispersion and SDS was introduced immediately prior to DGU. Details regarding the experimental procedures are described in the Methods section. We outline the framework of the separation mechanism before addressing the experimental results.

Co-Surfactant DGU Separation Mechanism. The first critical aspect of our proposed mechanism is recognizing that the morphology of the surfactants surrounding the SWNT can change during the entire DGU process. The extent of this change is related to the affinities between the SWNT and the surfactants present in the local environment, and the dynamic equilibrium state between the surfactants absorbed onto the nanotubes and free surfactant molecules present in the surrounding environment.[21-23,25,28] The exchange of surfactants occurs throughout the dispersion step and continues during the subsequent DGU separation process. Changes in the surfactant-SWNT micelle can be elucidated from optical spectra obtained at different stages of DGU separation, which will be discussed later.

The second critical aspect of this model is considering the significant contribution of the hydration layer to the overall buoyant density of surfactant-SWNT micelles.[24,29] The importance of this can be revealed by comparing DGU results performed using D_2O and H_2O (see Figure S4, Supporting Information). In addition to the large difference between the partial specific volumes of anhydrous and hydrated surfactants,[24] the different hydration conditions result in DOC-wrapped SWNTs having a much thicker hydration layer than SDS-wrapped SWNTs.[30,31]

The results of the following DGU experiments can be explained by considering these two aspects and the roles of the two co-surfactants.

Case I: Insignificant Change in Surfactant Environment. The procedure for Case I is shown in Figure 1(a), where SWNTs are dispersed in both DOC and SDS, then injected into the density gradient medium so that their initial position is approximately the same as their final position after the separation. Hence, changes in the surfactant environment around the SWNTs are negligible. A linear density gradient profile is used, which is formed from three layers (1 mL each) of 20%, 30%, and 40% v/v iodixanol in D_2O. The SWNT dispersion was mixed with an equal volume of 30% iodixanol prior to injection into the density gradient column.

It has been demonstrated that initial dispersion of SWNTs in DOC, followed by DGU in a density gradient medium containing SDS results in diameter-dependent separation of SWNTs.[19,20] Here, we investigate the role of SDS during the DGU process. Trial 1 in Figure 1(b) corresponds to both SDS-I (SDS used for dispersing SWNTs) and SDS-II (SDS used in the density gradient) being absent, which resulted in no separation of the SWNTs (surfactant concentrations are shown in Figure 1(c)). Trial 2 shows that a similar result is obtained when SDS is present only during the dispersion step but absent in the density gradient. These results show that wrapping SWNTs by DOC only to achieve dispersion is insufficient, and the additional presence of SDS is required for diameter-dependent separation.

The influence of SDS on SWNT dispersion was investigated by changing the concentration of SDS-I while maintaining a constant concentration of SDS-II (1.5% w/v, the weight of surfactants in the density gradient medium to the volume of the medium). These results are shown in Trials 3-7 in Figure 1(b). All of these trials resulted in some separation, but increasing the concentration of SDS-I from 0% (SWNTs initially dispersed only by DOC) to 0.875% (w/v, the weight of surfactants for dispersing SWNTs to the volume of solution injected into density gradient) increasingly broadened the final separated region.[32] In addition to broadening of the separated region, the position of each layer also shifted downward with increasing SDS-I concentration, indicating an overall increase in the density of the surfactant-SWNT micelles due to increasing SDS-I concentration. Furthermore, since each successive layer contains SWNTs of increasing average diameter,[19] SDS must influence the surfactant-SWNT micelles in a manner that is diameter dependent. The highest concentrations of SDS-I (Trial 7 in Figure 1(b)) increase the density of the surfactant-SWNT micelles to such an extent that some of the larger-diameter nanotubes (in the green and yellow layers) sink down to the bottom of the density gradient column.

The broadening of the diameter-dependent separated region seen in Trials 3-7 in Figure 1(b) can also be realized by introducing SDS-I during an intermediate stage, as shown in Figure 2(a). In these experiments, SWNTs were initially dispersed using only DOC, and

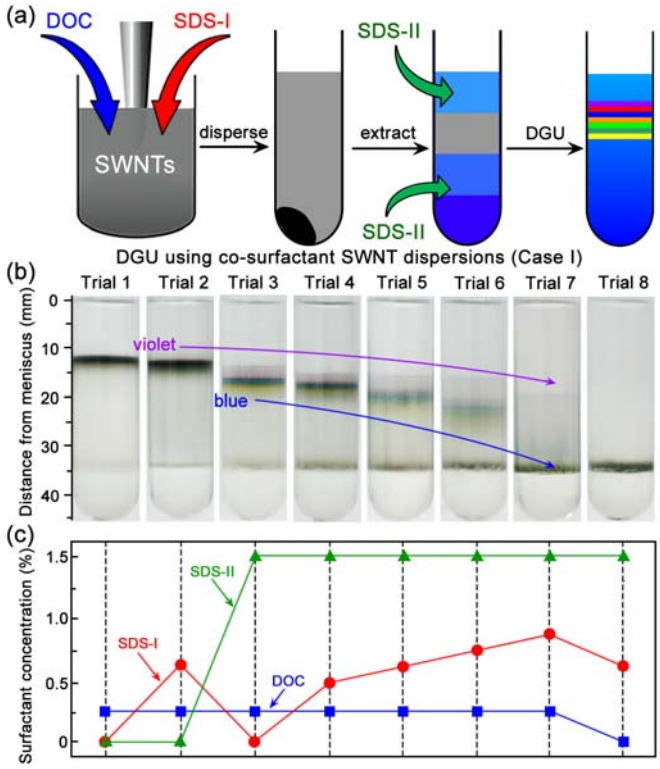

Figure 1. Density gradient ultracentrifugation results using co-surfactant SWNT dispersions for Case I. (a) Experimental procedures; (b) Realization and expansion of separated region using co-surfactants of DOC and SDS; (c) Corresponding co-surfactant recipes of these separations. See text for definition of SDS-I and SDS-II.

the supernatant was extracted after ultracentrifugation. SDS-I was then added to the DOC-dispersed SWNTs, and the mixture was injected into the previously described density gradient profile. This approach also resulted in diameter-dependent separation, but the expansion of the separated region was affected differently by the SDS-I concentration. Note in Figure 2(b) that some of the layers moved *upward* with increasing SDS-I concentration. Additionally, when compared with the procedure shown in Figure 1, similar expansions can be obtained with approximately the same concentration of SDS-I. Similar results were achieved by reversing the order, i.e. dispersing using SDS-I and then introducing DOC at the intermediate stage (see Figure S2, Supporting Information).

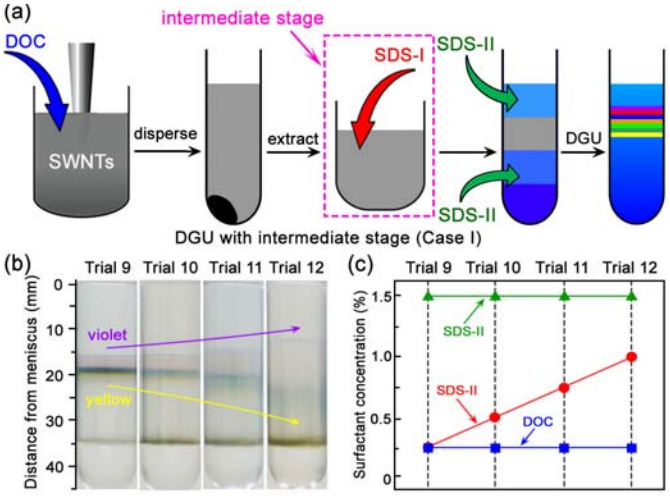

Figure 2. (a) DGU experimental procedure using intermediate stage for Case I; (b) Expansion of separated region by introduction of SDS at the intermediate stage; (c) Corresponding co-surfactant recipes of separations in (b).

Lastly, we note that no diameter-dependent separation can be achieved if DOC is absent from the dispersion step (Trial 8 in Figure 1(b)). This condition is known to result in separation by electronic type,[13] but requires a steeper density gradient to be observed (see the following section).

Case II: Changing Surfactant Environment. To investigate the role of surfactants during DGU, another density gradient profile was adopted, as shown in Figure 3(a). SWNTs were dispersed in DOC and SDS, and then placed on top of the density gradient column. As a result, the SWNT micelles must move down through the density gradient column during DGU in order to reach their isopycnic points. A steeper density gradient profile was necessary to observe the final separation, so a nonlinear density gradient column was used, which was formed from layers of 0.4 mL of 20%, 1 mL of 30%, 1 mL of 40%, and 0.6 mL of 60% v/v iodixanol in D_2O. Starting with the same DOC-SWNT dispersion as in Case I (SWNTs dispersed in 0.5% w/v DOC) and gradually increasing the concentration of SDS-I to

form a co-surfactant dispersion, different but related results were obtained. Surfactant concentrations are shown in Figure 3(c) (w/v, the weight of surfactants for dispersing SWNTs to the volume of solution injected into density gradient). The photograph in Figure 3(b) is representative of the resulting separation, in which we find two very different bands of SWNTs. The upper band is very narrow, and changes in both color and width according to SDS-I concentration (see Trials 13-16 in Figure 3(b)). For a pure DOC-SWNT dispersion (0% SDS-I) the thickness of this upper band is approximately 1 mm and appears to contain three different colored layers (Trial 13). These layers consist of small-diameter nanotubes, as revealed by the absorption spectra shown in Figure 3(b). A weak trend of increasing diameter is evident, reminiscent of the results obtained in the previously discussed cases. When the concentration of SDS-I is increased to 0.5% w/v the number of visible colored layers contained in this band decreases to only two, violet and red (Trial 14). The violet layer is highly enriched in (6,5) nanotubes, while the red layer contains primarily (6,5) and (7,5) nanotubes. These colors and corresponding (*n*,*m*) species are the same as those found for diameter-dependent separation of SWNTs in our previous report.[19] Further increasing the SDS-I concentration to 1.25% w/v results in more effective isolation of (6,5) nanotubes in this upper separation band and the disappearance of the red layer (Trial 15). Finally, when the SWNTs were dispersed only in SDS (0% DOC), no upper band was observed

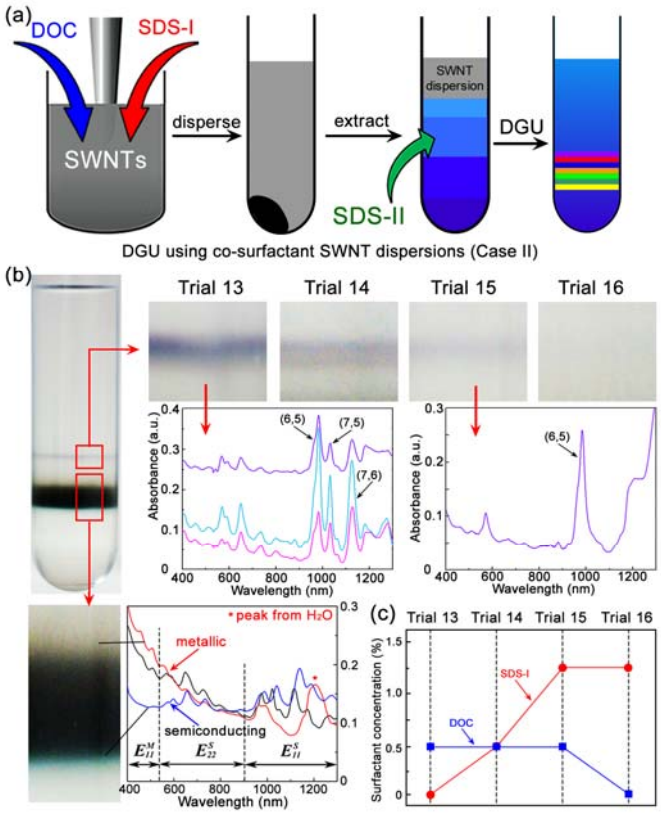

Figure 3. Density gradient ultracentrifugation results for Case II. (a) Experimental procedures; (b) Separation results in DGU column; (c) Surfactant recipes for these separations.

(Trial 16). This confirms the isolation of small-diameter SWNTs found in this upper band is achieved by DOC wrapping.

Approximately 4 mm below the thin upper band appears a wide, black band of what appears to be an unsorted collection of SWNTs. Careful inspection, however, reveals regions of blue and dark yellow extending below and above the unsorted region (see Figure 3(b)). Optical absorbance spectra obtained from these regions indicate the dark yellow region consists primarily of metallic SWNTs, while the blue region contains primarily semiconducting SWNTs, illustrating electronic-type separation. This separation is not as efficient as results previously reported by other groups,[11-13] thus the diameter distribution within the separated components cannot be determined.

We wish to draw attention to the trial in which SWNTs are initially dispersed only by SDS, which has no upper separation band but results in electronic type separation in the lower band (Trial 16). Since only SDS is involved during this entire process, the SWNT-micelles can only be comprised of SDS at all stages of this separation. The density of the SDS-SWNT micelles in the initial dispersion is approximately 1.1 g/mL, whereas the final densities are approximately 1.13 g/mL for metallic SWNTs and 1.23 g/mL for semiconducting SWNTs. This suggests that the SDS micelles change considerably during DGU, and the final micelles are significantly denser than in the initial dispersion. Moreover,

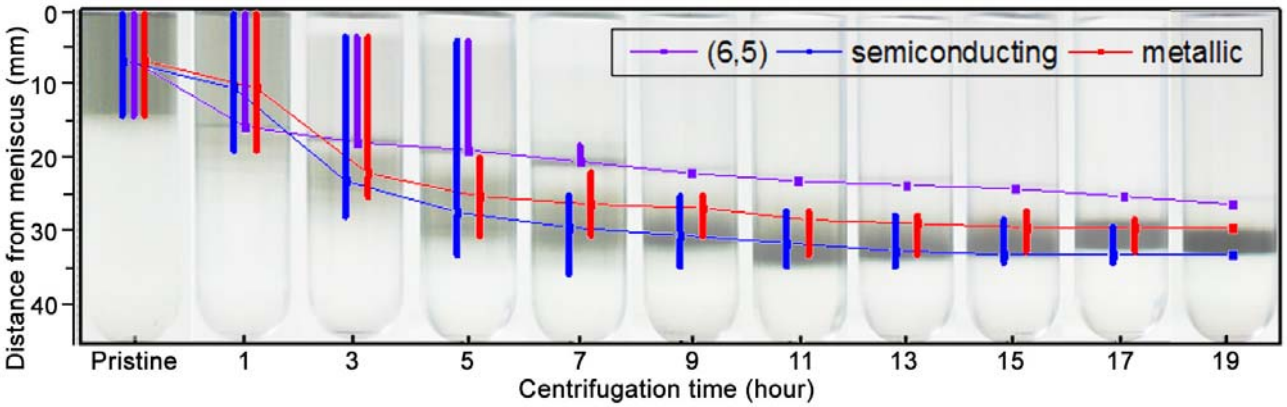

Figure 4. Time-dependent evolution of DGU separation starting with SDS/DOC co-surfactant dispersed SWNTs (Trial 15). The trace of the three primary separated components, violet, metallic, and semiconducting layers, are marked as a function of time. The bar indicates the apparent spread of the band, and the line connects the positions at which the band appears most concentrated.

compared with Trial 8 in Figure 1(b), the realization of such separation in Trial 16 is due to the appropriate steepness of the density gradient profile used in Case II.

The time-dependent evolution of Trial 15 in the Figure 3(b) separation is shown in Figure 4. This was performed using a co-surfactant SWNT dispersion of 0.5% w/v DOC and 1.25% w/v SDS, and evaluated every two hours. The distribution ranges of the violet, dark yellow, and blue components are indicated by vertical bars, and the positions of highest apparent concentration (i.e., richest color) are connected by a line. Emergence of the violet (6,5) layer from the pristine material occurs very quickly, requiring only about one hour of DGU. This suggests the difference between initial and final surfactant-SWNT micelle morphologies is small, presumably due to little exchange between DOC and SDS. After 9 hours, the violet layer reaches its isopycnic point and its shape becomes unchanging. Separation by electronic type, however, requires at least 15 hours to observe even slight changes indicating metallic/semiconducting enriched regions above/below the non-dispersed SWNTs. Results similar to those for Case II can also be realized by introducing SDS-I during an intermediate stage, as shown in Figure S5 in Supporting Information.

Importance of the Surfactant Environment. The preceding results cannot be explained in a consistent fashion without considering the surfactant environment during DGU. A comparison of the two density gradient profiles, as well as the initial and final positions of the SWNTs used in the above two cases are shown in Figure 5. In Case I, the final separation is in the same region as where the dispersion was initially injected (see Methods). Since the SWNTs remain in this region, they are surrounded by both DOC and SDS throughout the

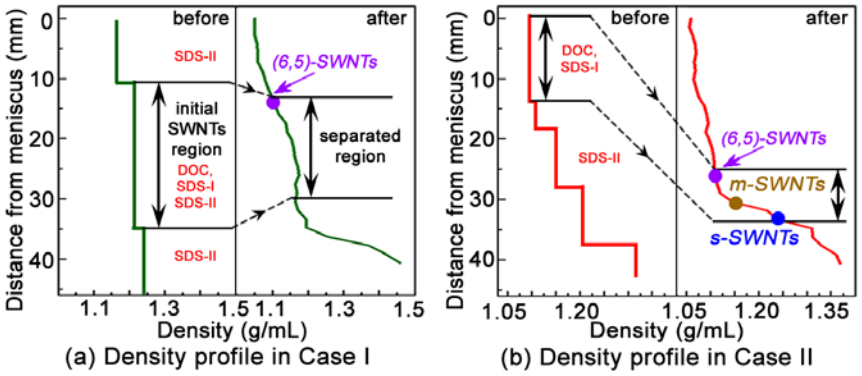

Figure 5. Density profiles in (a) Case I and (b) Case II before and after DGU process. Initial dispersion and post-DGU regions are marked.

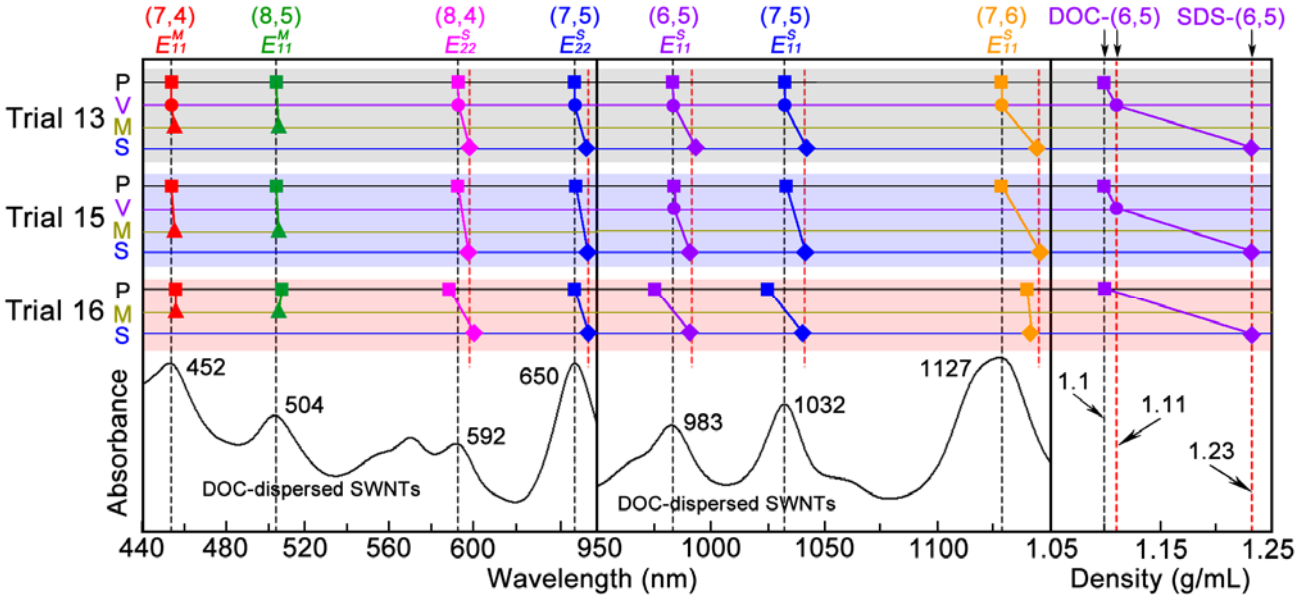

Figure 6. Optical absorption peak positions from several metallic and semiconducting chiralities and dispersion densities (right). Absorbance of DOC-dispersed SWNTs is shown at the bottom as a standard reference. Background colors of gray, blue and red indicate Trials 13, 15 and 16, respectively, and horizontal lines with different colors indicate different separated layers, as indicated on the left axis (P: pristine, V: violet, M: metallic, S: semiconducting). Average densities of (6,5) nanotubes enriched in different separated layers are shown on the right. Their different densities suggest different micelle morphologies. Vertical red dashed lines indicate shifted positions of those data.

entire DGU process. In contrast, the SWNT dispersion was placed on top of the density gradient column in Case II. Hence, the SWNTs had to move down through the density gradient column during DGU. In doing so, they moved from a DOC-rich environment into an SDS-rich environment, which significantly affects the morphology and composition of the surfactant-SWNT micelles. These changes can be elucidated from optical spectra of the various separated layers.

Density and absorbance information from DGU processes of Trial 13, 15 and 16 in Case II is shown in Figure 6, and is compared with different separated components from previous trials in Case I. For example, all the violet layers that appeared in these experiments have slightly different buoyant densities, ranging from approximately 1.1 to 1.15 g/mL. Considering the similar densities and absorbance intensities of these violet layers, the (6,5) species in these layers should have similar surfactant wrapping morphologies. When the density increases, however, the center position of the E_{11}^{S}

peak for (6,5) SWNTs in the dispersion also slightly increases from 983 to 985 nm. In initial DOC-SWNT dispersions and SDS-SWNT dispersions this value is 983 nm and 976 nm, respectively. For the semiconducting layers separated in lower band in Trials 13-16, the (6,5) species has a very large peak shift, and is located at 990±1 nm for DGU starting with SDS-SWNT dispersion (Trial 16) and co-surfactant dispersion (Trial 14, 15), and 994 nm for DGU using DOC-SWNT dispersion (Trial 13).

Similar results can be found for (7,5) nanotubes. From optical absorbance information of time-dependent analysis of Trial 15 in Case II (shown in Figure 4), in Figure 7 we plot the (7,5) E_{11} peak position from different DGU fractions extracted every two hours. In pristine co-surfactant dispersions of SWNTs (0.5% w/v DOC and 1.25% w/v SDS), the E_{11} for (7,5) SWNTs is located at 1033 nm, essentially the same as for pure DOC-SWNT dispersions (E_{11}=1032 nm). During DGU, however, the peak position increases as the SWNTs move down through the column into a more SDS-rich region, with the final position being 1042 nm. In electronic type separation by pure SDS-SWNT dispersion, this final value is 1040 nm. Hence, as the micelle changes from pure DOC to pure SDS the E_{11} peak position will redshift, as we observe along the column. This shows that the SWNTs are moving out the DOC-rich region, which is why the lower separation band has the same result as dispersion in pure SDS despite the initial presence of DOC. The one exception, however, is the small-diameter near-armchair

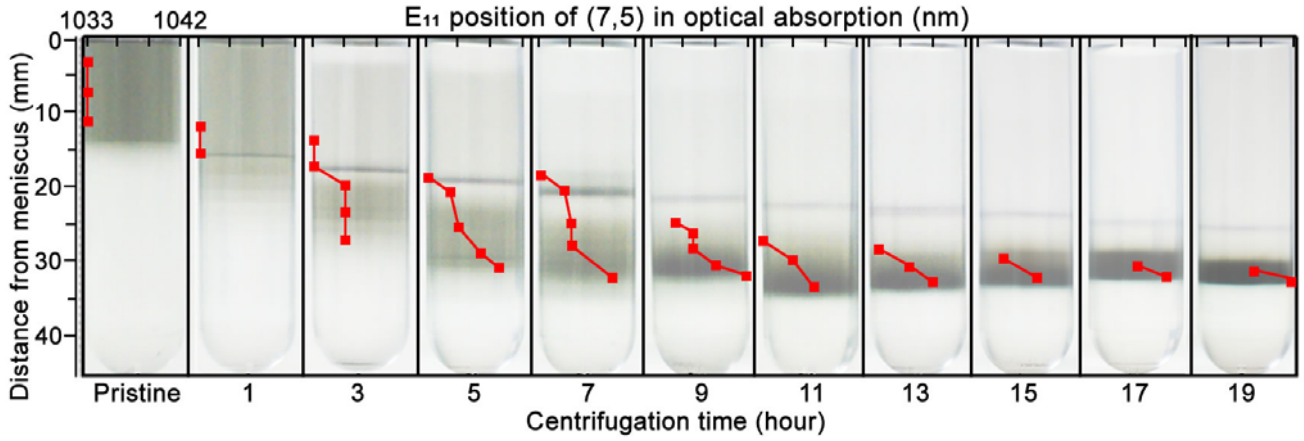

Figure 7. E_{11} position of (7,5) nanotubes in Trial 15 during time-dependent separation in Case II. All ten columns have the same wavelength unit for the upper axis (from 1033 to 1042 nm) as shown in pristine column.

SWNTs that remain in the upper band, especially (6,5). Due to the strong affinity of DOC to such SWNTs, the DOC micelle will not be completely replaced by SDS. These DOC-wrapped small-diameter SWNTs comprise the thin upper band seen in Case II.

Detailed Separation Mechanism Behind Case I and Case II. In Case I, the surfactant environment undergoes little change, with similar initial and final densities. Thus, excess DOC and SDS molecules in the initial dispersions, as well as SDS molecules contained in the density gradient of this area, are always available to the injected SWNT micelles. The structures of these initial surfactant-SWNT micelles are mainly cored by DOC-SWNT structures, and SDS molecules load onto the available space between DOC molecules.[19] This increases the mass of the micelles. However, this has a minimal effect on the micelle volumes since hydrated SDS molecules are considerably smaller than hydrated DOC molecules, leading to an enhancement of buoyant density differences in these nanotube micelles. Because of the low affinity of SDS with SWNTs, a sufficiently high concentration of SDS in the density gradient is critical to help stabilize the surfactant-SWNT micelles. This is the role of SDS-II shown in Trial 2 of Figure 1(b).

When the concentration of SDS in the initial dispersion increases, the morphologies of the surfactant-SWNT micelles will change. The change depends primarily on the relative affinities between the surfactants and the SWNTs. DOC-wrapped small-diameter SWNTs are stable even at higher SDS concentration because of the higher affinities to DOC molecules than to SDS molecules; the increased SDS concentration only increases the loading of SDS onto the space between DOC molecules. This increases the densities of these surfactant-SWNT micelles, leading to a slight downwards shift in the DGU column (e.g., the violet layer). For larger diameter nanotubes, however, their affinities with DOC is considerably lower, thus more SDS molecules will replace the absorbed DOC molecules and reduce the hydrated volume of the surfactant-SWNT micelle. The buoyant densities of these nanotubes will thus increase and shift downward with increasing SDS concentration, as seen in Figure 2(b). Moreover, if SDS is introduced later in the process, as in Figure 2(b), the process of changing from DOC-

wrapped SWNTs to SDS-loaded DOC-wrapped SWNTs is slower than the diffusion of the density gradient medium, causing low-density nanotubes to shift upwards instead of downwards.

The final micelle morphology in Case I will be determined by the ratio of initially present DOC molecules to added SDS molecules. The addition of SDS will serve to either replace DOC or attach to the pre-existing DOC-wrapped SWNTs, but the ratio of those two structures depends on the competition between the two surfactants.

In Case II, the initially dispersed SWNTs are placed at the top of the density gradient and then move downward during DGU until reaching their isopycnic point in the middle part of the column. The resulting change in surfactant environment between the initial position (both DOC and SDS present) and final position (only SDS present) leads to a more significant change in the SWNT micelles than for Case I.

The most significant result seen in trials of Case II is that in addition to the separation of metallic and semiconducting nanotubes, which evidently results from SDS (see Trial 16 in Figure 3(b)), small-diameter nanotubes are simultaneously isolated. Take Trial 13 as an example, which starts with SWNTs dispersed by DOC. When the DOC-SWNT micelles move downward through the column they move from a DOC-rich environment into an SDS-rich environment. For large-diameter nanotubes, DOC will gradually be replaced by SDS, and the nanotube-micelle hydration-layer sizes will be reduced. This increases the micelle density and results in separation by electronic type. However, for small-diameter (especially near-armchair) nanotubes the DOC-SWNT structure survives because of the

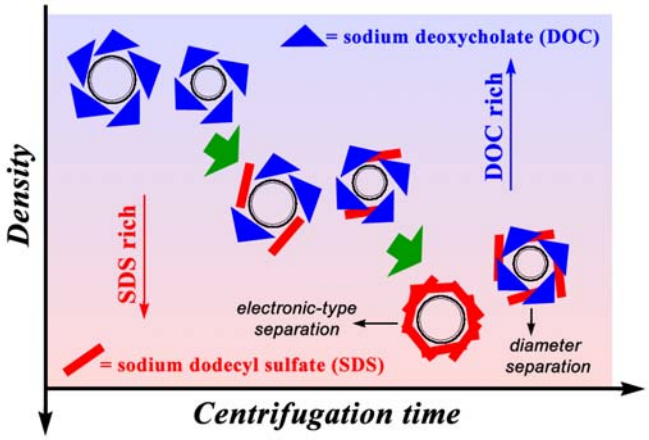

Figure 8. Wrapping structures of different nanotubes under different co-surfactant environments.

high affinity with DOC molecules. This leads to the diameter-dependent separation observed in the upper region, in which the densities of the small SWNT micelles are almost the same as in the diameter-dependent expansion described in Figure 1 and Figure 2. See Figure 8 for structures of these surfactant-SWNT micelles in different surfactant environments.

Conclusion

Although both DOC and SDS can be used to effectively disperse SWNTs, the results of DGU-based separation using such SWNT micelles can yield quite different results. Moreover, because of the unequal affinities of different surfactants, surfactant-SWNT micelles can change morphology based on the local surfactant environment while moving through the density gradient. Here we present a model describing surfactant encapsulation of SWNTs by DOC and SDS that explains DGU separation results starting with co-surfactant SWNT dispersions. Although our experiments were conducted using DOC and SDS co-surfactants, we believe our discussion and model should extend to bile salts and anionic salts in general. We also demonstrate that the initial position of the SWNT dispersion in the density gradient is important because the local surfactants contained in the starting dispersion can affect the micelle morphologies if they differ from those contained in the rest of the density gradient. The affinities of different surfactants are critical in determining the final morphologies and sizes of the micelles when they reach an equilibrium state. Therefore, by designing a proper density gradient,[33] results of DGU experiments can be predicted before they are performed, significantly improving the effectiveness of the DGU technique and obtaining the desired separation.

Methods

The nanotubes used in these experiments were synthesized by the alcohol catalytic chemical vapor deposition (ACCVD) method.[34] These SWNTs more effectively reveal the efficacy of the DGU process due to the broader diameter distribution compared to other commercially available SWNTs (e.g.,

CoMoCAT). Furthermore, ACCVD SWNTs tend to have a narrower chirality distribution[35] than HiPCO SWNTs, thus are more easily analyzed. The SWNTs were dispersed in either DOC or SDS surfactant by ultrasonication for 30 min at 400 W/cm^2 using a horn-type ultrasonicator (UP-400s, Hielscher Ultrasonics). The dispersion was then immediately centrifuged at 276,000 *g* for 15 min while maintained at a temperature of 22 °C. The upper 80% of the supernatant was carefully decanted. In Case I, it was diluted by iodicanol stock (OptiPrep^{TM} density gradient medium, Sigma-Aldrich Co., Ltd.) to a sample layer with 30% iodixanol, while in Case II, the decanted supernatant was directly used as sample layer. A density gradient column was formed separately inside a 5 mL polycarbonate centrifuge tube (approx. 1.3 cm diameter, 5.2 cm in length) by layering different concentrations of iodixanol-water solutions. The two density gradient profiles used in our DGU experiments are as follows: in Case I it contained 1 mL each of 20%, 30%, and 40% v/v iodixanol in D_2O, whereas in Case II contained 0.4 mL of 20%, 1 mL of 30%, 1 mL of 40%, and 0.6 mL of 60% v/v iodixanol in D_2O. In some experiments, DOC and/or SDS were also introduced into the density gradient medium at different concentrations (see Supporting Information). After layering, the density gradient column was placed horizontally and allowed to diffuse for 1 h in order to create a smooth density gradient profile. The sample layer of the SWNT dispersion was then carefully injected at a point where its density approximately matched that of the density gradient (Case I) or placed on top of the density gradient (Case II). The columns were then ultracentrifuged at 197,000 *g* using a Hitachi-Koki S52ST swing-bucket rotor. After centrifugation, gradient linearization was achieved and each of the resulting layers was extracted and collected using a micropipette. Please see Supporting Information for details regarding SWNT separation. UV-Vis-NIR absorbance spectra (UV-3150 spectrometer, Shimadzu) and photoluminescence excitation spectra[36] (HORIBA Fluorolog IHR 320, equipped with a liquid-nitrogen-cooled GaAs detector) of the fractionated samples were then measured and analyzed.

Acknowledgement. Part of this work was financially supported by Grant-in-Aid for Scientific

Research (22226006 and 19054003), NEDO (Japan), ‘Development of Nanoelectronic Device Technology’ of NEDO, and Global COE Program ‘Global Center for Excellence for Mechanical Systems Innovation’. PZ acknowledges a scholarship granted by the China Scholarship Council, and GL acknowledges support from the NanoJapan program funded by the National Science Foundation.

Supporting Information Available: Experimental details, optical information from different DGU experiments, simple model calculation, calculated density profiles using the Lamm Equation, and some other DGU results mentioned in the text. This material is available free of charge via the Internet at http://pubs.acs.org.

References:

(1) Carbon Nanotubes: Advanced Topics in the Synthesis, Structure, Properties and Applications (Topics in Applied Physics); Jorio, A., Dresselhaus, G., Dresselhaus, M. S., Eds.; Springer: New York, 2008.

(2) Usrey, M. L.; Lippmann, E. S.; Strano, M. S. Evidence for a Two-Step Mechanism in Electronically Selective Single-Walled Carbon Nanotube Reactions. *J. Am. Chem. Soc.* **2005**, *127*, 16129-16135.

(3) Krupke, R.; Hennrich, F.; Löhneysen, H. V.; Kappes, M. M. Separation of Metallic from Semiconducting Single-Walled Carbon Nanotubes. *Science* **2003**, *301*, 344-347.

(4) Banerjee, S.; Hemraj-Benny, T.; Wong, S. S. Covalent Surface Chemistry of Single-Walled Carbon Nanotubes. *Adv. Mater*. **2005**, *17*, 17-29.

(5) Chen, Z.; Du, X.; Du, M.; Rancken, C. D.; Cheng, H.; Rinzler, A. G. Bulk Separative Enrichment in Metallic or Semiconducting Single-Walled Carbon Nanotubes. *Nano Lett*. **2003**, *3*, 1245-1249.

(6) Arnold, M. S.; Stupp, S. I.; Hersam, M. C. Enrichment of Single-Walled Carbon Nanotubes by

Diameter in Density Gradients. *Nano Lett.* **2005**, *5*, 713-718.

(7) Arnold, M. S.; Green, A. A.; Hulvat, J. F.; Stupp, S. I.; Hersam, M. C. Sorting Carbon Nanotubes by Electronic Structure using Density Differentiation. *Nature Nanotech.* **2006**, *1*, 60-65.

(8) Zheng, M.; Jagota, A.; Strano, M. S.; Santos, A. P.; Barone, P.; Chou, S. G.; Diner, B. A.; Dresselhaus, M. S.; Mclean, R. S.; Onoa, G. B. *et al.* Structure-Based Carbon Nanotube Sorting by Sequence-Dependent DNA Assembly. *Science* **2003**, *302*, 1545-1548.

(9) Ju, S.-Y.; Doll, J.; Sharma, I. Papadimitrakopoulos, F. Selection of Carbon Nanotubes with Specific Chiralities Using Helical Assemblies of Flavin Mononucleotide. *Nature Nanotech.* **2008**, *3*, 356-362.

(10) Nish, A.; Hwang, J.-Y.; Doig, J.; Nicolas, R. J. Highly Selective Dispersion of Single-Walled Carbon Nanotubes Using Aromatic Polymers. *Nature Nanotech.* **2007**, *2*, 640-646.

(11) Green, A. A.; Hersam, M. C. Colored Semitransparent Conductive Coatings Consisting of Monodisperse Metallic Single-Walled Carbon Nanotubes. *Nano Lett.* **2008**, *8*, 1417-1422.

(12) Yanagi, K.; Miyata, Y.; Kataura, H. Optical and Conductive Characteristics of Metallic Single-Wall Carbon Nanotubes with Three Basic Colors; Cyan, Magenta, and Yellow. *Appl. Phys. Express* **2008**, *1*, 034003/1-034003/3.

(13) Niyogi, S.; Densmore C. G.; Doorn, S. K. Electrolyte Tuning of Surfactant Interfacial Behavior for Enhanced Density-Based Separations of Single-Walled Carbon Nanotubes. *J. Am. Chem. Soc.* **2009**, *131*, 1144-1153.

(14) Chernov, A. I.; Obraztsova, E. D. Metallic Single-Wall Carbon Nanotubes Separated by Density Gradient Ultracentrifugation. *Phys. Stat. Sol. (b)* **2009**, *246*, 2477-2481.

(15) Hennrich, F.; Arnold, K.; Lebedkin, S.; Quintillá, A.; Wenzel, W.; Kappes, M. M. Diameter Sorting of Carbon Nanotubes by Gradient Centrifugation: Role of Endohedral Water. *Phys. Stat. Sol. (b)* **2007**, *244*, 3896-3900.

(16) Wei, L.; Lee, C. W.; Li, L. -J.; Sudibya, H. G.; Wang, B.; Chen, L. Q.; Chen, P.; Yang, Y.; Chan-Park, M. B.; Chen, Y. Assessment of (n,m) Selectively Enriched Small Diameter Single-Walled Carbon Nanotubes by Density Differentiation from Cobalt-Incorporated MCM-41 for Macroelectronics. *Chem. Mater.* **2008**, *20*, 7417.

(17) Fleurier, R.; Lauret, J. -S.; Flahaut, E.; Loiseau, A. Sorting and Transmission Electron Microscopy Analysis of Single or Double Wall Carbon Nanotubes. *Phys. Stat. Sol. (b)* **2009**, *246*, 2675-2678.

(18) Green, A. A.; Duch, M. C.; Hersam, M. C. Isolation of Single-Walled Carbon Nanotube Enantiomers by Density Differentiation. *Nano Research* **2009**, *2*, 69-77.

(19) Zhao, P.; Einarsson, E.; Xiang, R.; Murakami, Y.; Maruyama, S. Controllable Expansion of Single-Walled Carbon Nanotube Dispersions Using Density Gradient Ultracentrifugation. *J. Phys. Chem. C* **2010**, *114*, 4831-4834.

(20) Ghosh, S.; Bachilo, S. M.; Weisman, R. B. Advanced Sorting of Single-Walled Carbon Nanotubes by Nonlinear Density Gradient Ultracentrifugation. *Nature Nanotech.* **2010**, *5*, 443-450.

(21) Wang, H.; Zhou, W.; Ho, D. L.; Winey, K. L.; Fischer, J. E.; Glinka, C. J.; Hobbie, E. K. Dispersing Single-Walled Carbon Nanotubes with Surfactants: A Small Angle Neutron Scattering Study. *Nano Lett.* **2004**, *4*, 1789-1793.

(22) Sasaki, Y.; Nagata, H. D.; Fujii, Y. -K.; Lee, S.; Nagadome, S.; Sugihara, G. A Thermodynamic Study on the Adsorption Behavior of Four Bile Salt Species on Graphite in Water. *Colloids Surf. B* **1997**, *9*, 169-176.

(23) Nair, N.; Kim, W.-J.; Braatz, R. D.; Strano, M. S. Dynamics of Surfactant-Suspended Single-Walled Carbon Nanotubes in a Centrifugal Field. *Langmuir* **2008**, *24*, 1790-1795.

(24) Arnold M. S.; Switivich, J.; Stupp, S. I.; Hersam, M. C. Hydrodynamic Characterization of Surfactant Encapsulated Carbon Nanotubes Using an Analytical Ultracentrifuge. *ACS Nano* **2008**, *2*, 2291-2300.

(25) Carvalho, E. J. F.; dos Santos, M. C. Role of Surfactants in Carbon Nanotubes Density Gradient Separation. *ACS Nano* **2010**, *4*, 765-770.

(26) Yurekli, K.; Mitchell, C. A.; Krishnamoorti, R. Small-Angle Neutron Scattering from Surfactant-Assisted Aqueous Dispersions of Carbon Nanotubes. *J. Am. Chem. Soc.* **2004**, *126*, 9902-9903.

(27) Richard, C.; Balavoine, F.; Schultz, P.; Ebbesen, T. W.; Miskowski, C. Supramolecular Self-Assembly of Lipid Derivatives on Carbon Nanotubes. *Science* **2003**, *300*, 775-778.

(28) McDonald, T. J.; Engtrakul, C.; Jones, M.; Rumbles, G.; Heben, M. J. Kinetics of PL Quenching during Single-Walled Carbon Nanotube Rebundling and Diameter-Dependent Surfactant Interactions. *J. Phys. Chem. B* **2006**, *110*, 25339-25346.

(29) O'Connell, M. J.; Bachilo, S. M.; Huffman, C. B.; Moore, V. C.; Strano, M. S.; Haroz, E. H.; Rialon, K. L.; Boul, P. J.; Noon, W. H.; Kittrell, C. *et al*. Band Gap Fluorescence from Individual Single-Walled Carbon Nanotubes. *Science* **2002**, *297*, 593-596.

(30) Fontell, K. Micellar Behaviour in Solutions of Bile-Acid Salts. *Kolloid-Z. u. Z. Polymere* **1971**, *244*, 246-252.

(31) Mukerjee, P. The Hydration of Micelles of Association Colloidal Electrolytes. *J. Colloid. Sci.* **1964**, *19*, 722-728.

(32) In Case I, the initial concentration of DOC used for dispersing SWNTs was 0.5% w/v (30 mg DOC in 6 mL D_2O). After SWNT supernatant was decanted and diluted by equal volume of iodixanol stock, this concentration was halved to 0.25% w/v, as shown in Figure 1. In Case II, because of the absence of dilution, the initial concentration will stay the same until placed on top of density gradient.

(33) Lamm, O. Die differentialgleichung der ultrazentrifugierung. *Ark. Mat. Astr. Fys* **1929**, *21B*, 1-4.

(34) Maruyama, S.; Kojima, R.; Miyauchi, Y.; Chiashi, S.; Kohno, M. Low-Temperature Synthesis

of High-Purity Single-Walled Carbon Nanotubes from Alcohol. *Chem. Phys. Lett*. **2002**, *360*, 229-234.

(35) Miyauchi, Y.; Chiashi, S.; Murakami, Y.; Hayashida, Y.; Maruyama, S. Fluorescence Spectroscopy of Single-Walled Carbon Nanotubes Synthesized from Alcohol. *Chem. Phys. Lett.* **2004**, *387*, 198-203.

(36) Bachilo, S. M.; Strano, M. S.; Kittrell, C.; Hauge, R. H.; Smalley, R. E.; Weisman, R. B. Structure-Assigned Optical Spectra of Single-Walled Carbon Nanotubes. *Science* **2002**, *298*, 2361-2366.

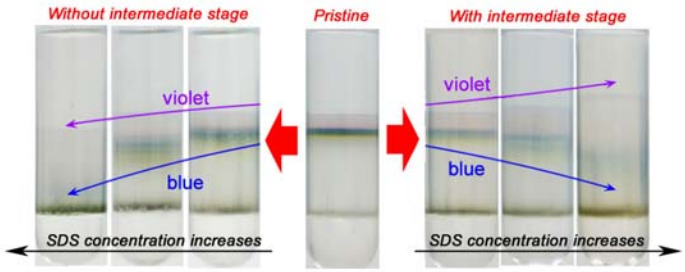
Without intermediate stage
Pristine
With intermediate stage
violet
blue
violet
blue
SDS concentration increases
SDS concentration increases

TOC Figure